

Energy and CO₂ exchanges and influencing factors in spring wheat ecosystem along the Heihe River, northwestern China

SHUCHEN SUN^{1,3}, MING'AN SHAO^{1,2,*} and HONGBEI GAO⁴

¹State Key Laboratory of Soil Erosion and Dryland Farming on the Loess Plateau, Institute of Soil and Water Conservation, Chinese Academy of Sciences and Ministry of Water Resources, Yangling, 712100, Shaanxi, China.

²Institute of Geographical Science and Natural Resources Research, Chinese Academy of Science, Beijing, 100049, China.

³University of Chinese Academy of Sciences, Beijing, 100049, China.

⁴Shaanxi Provincial Land Engineering Construction Group Co. Ltd., Xi'an, Shaanxi, 710075, China.

*Corresponding author. e-mail: mashao@ms.iswc.ac.cn

Spring wheat (*Triticum aestivum* Linn.) is an important crop for food security in the desert-oasis farmland in the middle reaches of the Heihe River in northwestern China. We measured fluxes using eddy covariance and meteorological parameters to explore the energy fluxes and the relationship between CO₂ flux and climate change in this region during the wheat growing seasons in 2013 and 2014. The energy balance closures were 70.5% and 72.7% in the 2013 and 2014 growing season, respectively. The wheat ecosystem had distinct seasonal and diurnal dynamics of CO₂ fluxes with U-shaped curves. The accumulated net ecosystemic CO₂ exchanges (NEE) were -111.6 and -142.2 g C/m² in 2013 and 2014 growing season, respectively. The ecosystem generally acted as a CO₂ sink during the growing season but became a CO₂ source after the wheat harvest. A correlation analysis indicated that night-time CO₂ fluxes were exponentially dependent on air temperature and soil temperature at a depth of 5 cm but were not correlated with soil-water content, water-vapour pressure, or vapour-pressure deficit. CO₂ flux was not correlated with the meteorological parameters during daytime. However, irrigation and precipitation, may complicate the response of CO₂ fluxes to other meteorological parameters.

1. Introduction

Weather and climate change on Earth are not only driven by the amount and distribution of solar radiation (Trenberth *et al.* 2009), but are also influenced by terrestrial ecosystemic processes, such as the exchanges of energy, CO₂, and water between land surfaces and the atmosphere (Pielke *et al.* 1998; Patil *et al.* 2014). Investigating exchanges of energy and CO₂ under a variety of terrestrial ecosystems is thus very important for understanding the mechanisms that control these exchanges.

The development of micrometeorological techniques, especially methods that measure eddy covariance (EC), has provided a new way to investigate the exchanges of carbon, water and energy between land surface and the atmosphere. So far, many studies of the exchanges of energy and CO₂ under different ecosystems have been reported, such as forests, grassland, cropland, and wetland (Hunt *et al.* 2004; Admiral *et al.* 2006; José *et al.* 2007; Jiang *et al.* 2014; Jing *et al.* 2014; Ohta *et al.* 2014; Posse *et al.* 2014; Tyagi *et al.* 2014; Zeri *et al.* 2014). Most of these studies have been

Keywords. Eddy covariance; energy and CO₂ fluxes; desert-oasis ecotone; spring wheat.

conducted in temperate or tropical climates, and few studies have been conducted in arid or semi-arid regions (Yuan *et al.* 2014; Vote *et al.* 2015), especially in desert-oasis farmland. Arid and semi-arid regions cover approximately 40% of Earth's land surface (Schimel 2010) and so contribute substantially to Earth's climatic system (Rotenberg and Yakir 2010) and are significantly affected by agricultural activities (Spiertz 2012). However, the contribution of arid and semi-arid agricultural ecosystems to the carbon cycle as net sources or sinks of CO₂ remains poorly known (Vote *et al.* 2015). But higher atmospheric CO₂ levels have significant effects on crop plants, such as by altering crop physiology and productivity (Khan and Hanjra 2009; Yu *et al.* 2012). Morgan *et al.* (2011) reported that the soil-water content and productivity may be higher than previously expected in semi-arid grasslands under a warmer and CO₂-enriched environment.

Oases are important foci of agricultural land in the middle reaches of the Heihe River in northwestern China and can provide enough food for the local population and livestock. Oases have different shapes and sizes and coexist within widespread deserts (Cheng *et al.* 1999) and usually form naturally in the deltas of inland rivers or on alluvial-diluvial plains and the edges of alluvial-diluvial fans. Native deserts, however, have been converted in recent decades to irrigated cropland due to the nutritional and economic demands of the growing population (Li *et al.* 2006). Changes in land use will affect local surface exchanges of mass and energy (Foley *et al.* 2005; Scott *et al.* 2012), e.g., lower rainfall, reduced runoff, and decreased water availability (Intergovernmental Panel on Climate Change 2007). Reichstein *et al.* (2002) and Ivans *et al.* (2006) reported that some extreme events, such as rainstorms or droughts, often strongly influence the surface fluxes of energy and CO₂ due to the water-limitation and lower precipitation in arid and semi-arid regions. Practices of irrigation management can also strongly influence the distribution of turbulent fluxes in semi-arid regions (Vote *et al.* 2015). Thus, investigating the exchanges of energy and CO₂ between land surfaces and the atmosphere is very important for sustainable development of the oases.

This study was conducted in a field of spring wheat in an oasis of the Heihe River using an EC system to investigate energy and CO₂ exchanges between the land surface and the atmosphere. Our aims were (1) to investigate the daily and seasonal variation in energy and CO₂ fluxes and (2) to examine the factors controlling CO₂ fluxes in a typical desert-oasis farmland. The results of this study will improve our understanding of land-surface processes in desert-oasis farmland.

2. Materials and methods

2.1 Site description

The study site was in typical farmland of the desert-oasis ecotone (39°23'N, 100°1'E, 1370 m asl) of Linze County in the middle reaches of the Heihe River in northwestern China (figure 1). This area has a typical desert climate characterised by aridity, high solar radiation, and frequent strong winds (mean annual wind speed is 3.2 m s⁻¹, with winds mainly from the northwest). Mean temperature is 7.6°C, with a maximum and minimum of 39.1 and -27.8°C in July and January, respectively. Mean annual precipitation is 119 mm, approximately 65% of which falls from July to September, and mean annual pan evaporation is 2390 mm (Zhang and Shao 2013; Li and Shao 2014). The typical cropping system in this region consists of yearly maize (*Zea mays* L.), spring wheat (*Triticum aestivum* Linn.), tomatoes (*Solanum lycopersicum*), cotton (*Gossypium* spp.), and sugar beets (*Beta vulgaris*).

In our study, the wheat was planted in Mid-March and harvested in Mid-July. The growing period was about 4 months (~120 days). Irrigation was required four or five times (140–160 mm each time) during the growing season depending on the management of the water supply and on drought conditions. Winter irrigation is needed after harvest and generally in late October or early November to prevent the soil from freezing, to restrict evaporation from the soil, and to ensure normal conditions for the next year. The soil in this region is a sandy loam, with an average bulk density and field water capacity of 1.40 g/cm³ and 20.43%, respectively.

2.2 Environmental variables and flux measurement

Air temperature (T_a) and relative humidity were measured by a humidity/temperature probe (HMP155, Vaisala, Helsinki, Finland) installed 1.5 m above the ground. All downward and upward radiation were measured at a height of 1.5 m using a CRN4 net radiometer (Kipp & Zonen, Delft, Netherlands). Soil temperature (T_s) and soil volumetric water content (SWC) were measured at depths of 5, 10, 20, 40, and 60 cm using temperature probes (Model 109ss, Campbell Scientific Inc.) and time domain reflectometry (TDR) soil-moisture sensors, respectively. Soil heat fluxes (G) were measured at depths of 5 and 10 cm by two heat-flux plates (HFP01-L, Campbell Scientific). All these variables were collected as half-hourly averages and stored by a data logger (CR1000, Campbell Scientific). Precipitation (P) data were from the Linze Inland River Basin Research

Station, Chinese Ecosystem Research Network, approximately 15 km from the study site.

Sensible heat, latent heat, and CO₂ fluxes between the land surface and the atmosphere were measured continuously from April to July 2013 and from March to July 2014 by an EC system installed 2.2 m above the ground (figure 1). The system was composed of an open-path infrared CO₂/H₂O gas analyser (IGRA, Model LI-7500A, LI-COR, USA) and a three-dimensional sonic anemometer (CSAT3, Campbell Scientific). The distance between the IGRA and CSAT3 was 10 cm. Raw data from the IGRA and CSAT3 were obtained at a frequency of 10 Hz and stored in a data logger (CR3000, Campbell Scientific).

2.3 Calculations and data processing

2.3.1 Surface energy balance

The energy balance was calculated by:

$$R_n - G_s = H_s + LE \quad (1)$$

where R_n is the net radiation, G_s is the soil heat flux at the surface, H_s is the sensible heat flux, and LE is the latent heat flux. Energy balance closure (EBC) was calculated using a linear regression as the half-hourly $(H_s + LE)$ vs. $(R_n - G_s)$. G_s are given by:

$$G_s = G_5 + S \quad (2)$$

where G_5 is the soil heat flux measured by a heat plate at a depth of 5 cm, and S is the heat storage

in the 5 cm of soil above the heat flux plate. The soil heat storage flux was calculated as (Oliphant *et al.* 2004):

$$S = \frac{\Delta T_s C_s d}{\Delta t} \quad (3)$$

$$C_s = \rho_b C_d + \theta_v \rho_w C_w \quad (4)$$

where ΔT_s is the average soil temperature above the heat flux plate, d is the thickness of the soil above the heat flux plate, Δt is the time, C_s is the heat capacity of moist soil, ρ_b is the bulk density of the soil, C_d is the heat capacity of a dry mineral soil (in this case, $C_d = 840$ J/kg K, Hanks and Ashcroft 1980), ρ_w is the density of water, θ_v is the volumetric SWC measured by TDR soil-moisture sensors, and C_w is the heat capacity of water.

The energy balance ratio (EBR) was also used to evaluate the quality of the EC data. The EBR was calculated by (Wilson and Baldocchi 2000; Tsai *et al.* 2007):

$$EBR = \frac{\sum (H_s + LE)}{\sum (R_n - G_s)} \quad (5)$$

2.3.2 CO₂ flux and gap filling

Half-hourly CO₂ flux data were rejected in accordance with the criteria: (1) incomplete half hourly data, (2) data influenced by rainfall, and the subsequent 2 hr, and sensible and latent heat

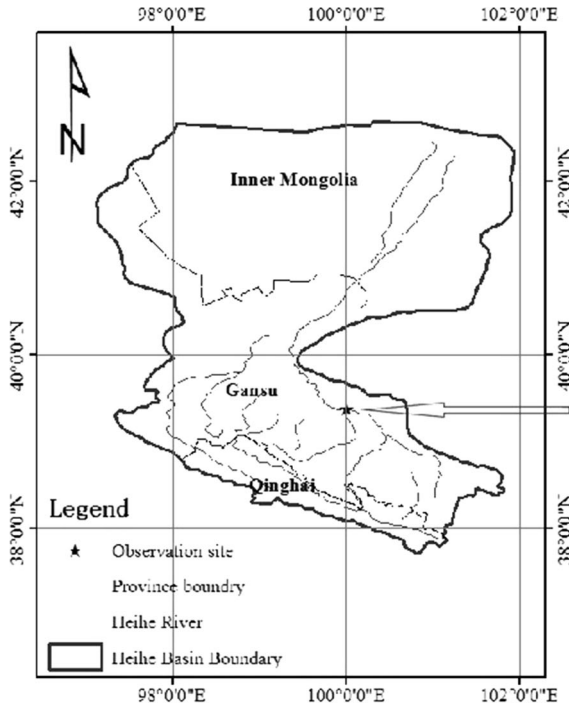


Figure 1. Location and study site.

fluxes were excluded, (3) the fluxes under stable night-time conditions when friction velocity (u^*) was <0.15 m/s, and (4) data with spikes. Approximately 28.7% and 28.4% of the data in the 2013 and 2014 growing seasons, respectively, were lost due to power failures, instrument malfunction, or the above criteria.

Linear interpolation was used to fill small gaps within 2 hr (Aubinet *et al.* 2000). Daytime mean diurnal variation (Falge *et al.* 2001) was applied for gaps >2 hr using data windows of 14 days. All raw EC fluxes were processed using Eddy Pro 5.2.0 (LI-COR, Lincoln, Nebraska, USA).

Net ecosystemic respiration (R_{eco}) at night was equal to net CO_2 flux (F'_c) at night due to the absence of photosynthetic activity as (Ohta *et al.* 2014; Vote *et al.* 2015):

$$R_{\text{eco}} = F'_c \quad (6)$$

where R_{eco} is the night-time net ecosystemic respiration and F'_c is the net CO_2 flux during the night-time. Due to R_{eco} is sensitive to temperature (Lloyd and Taylor 1994), a simple exponential function was found between F'_c and soil temperature (Leuning *et al.* 2005):

$$F'_c = a \exp(bT_s) \quad (7)$$

where a and b are empirical constants, and T_s is the soil temperature at a depth of 5 cm. This exponential function was then used to calculate daytime R_{eco} .

The relationship among net ecosystemic CO_2 exchanges (NEE, $\text{g C/m}^2 \text{ d}$) by the eddy covariance system ($\text{g C/m}^2 \text{ d}$), gross primary production (GPP, $\text{g C/m}^2 \text{ d}$), and R_{eco} ($\text{g C/m}^2 \text{ d}$) is:

$$\text{NEE} = -\text{GPP} + R_{\text{eco}}. \quad (8)$$

3. Results

3.1 Meteorological variation

The variations of meteorological conditions during the study are shown in figure 2. Each parameter had a similar trend throughout both growing seasons. Mean T_a was 18.3 ± 5.3 and $16.7 \pm 6.0^\circ\text{C}$ in 2013 and 2014, respectively. The difference was due to the length of growth season. The total P was 76.6 and 50.2 mm in 2013 and 2014, respectively, mainly from day 160 to 200 (June–July) and especially in the middle of June and July. P was higher during the 2013 than the 2014 growing season and had a maximum of 27.8 mm on day 195 in 2013.

The daily mean T_s was consistent with T_a . The relationship between T_s and T_a can be described linearly as $T_s = 0.89T_a + 1.76$ ($R^2 = 0.86$, $p < 0.0001$). The mean T_s during the growing season were

18.2 ± 4.7 and $16.4 \pm 6.1^\circ\text{C}$ in 2013 and 2014, respectively. T_s were below 5°C at the beginning of the 2014 growing season until late March (from days 71 to 80, figure 2b). The SWC at a depth of 5 cm varied cyclically during the study, consistent with the periods of irrigation and precipitation (figure 2b). SWC will peak after each irrigation or rain and the peak value will depend on the amount of water added. SWC was higher when irrigation coincided with rain than after irrigation or precipitation individually, and the contribution of precipitation to the SWC was dependent on the background SWC and on the rainfall. For example, during the 2013 growing season when P reached 27.8 mm on day 195, the peak SWC value was similar to the previous peak with irrigation on day 182.

Since the daily mean vapour-pressure deficit (VPD) is calculated as the difference between saturation vapour and the daily mean water-vapour pressure (e), the two have to have opposite trends. Likewise, telling us that humidity increased when it was raining is also obvious.

3.2 Surface EBC

EBC has generally been used to test EC data (Mahrt 1998) and is a standard procedure for evaluating the data quality at some sites (Schmid *et al.* 2000; Wilson and Baldocchi 2000). Surface energy includes not only R_n , G , LE , and H_s , but also heat storage in the soil, plant biomass, and air under the instrument and the canopy. We included only the soil heat storage in our study due to the limitation of biometric data. The mean EBC of the wheat was 70.5 and 72.7% in 2013 and 2014, respectively, higher in 2014 than in 2013, but R^2 was lower in 2014 than in 2013 (figure 3). The EBR was 0.74 and 0.73 in 2013 and 2014, respectively, consistent with the findings by Stoy *et al.* (2013) who reported a mean EBR of 0.78 among cropping systems. Vote *et al.* (2015) reported a mean EBR for wheat of 0.61 in an Australian semi-arid climatic zone.

3.3 Dynamics of CO_2 fluxes

The dynamics of NEE, R_{eco} , and GPP had distinct seasonal trends during both growing seasons (figure 4 and table 1). NEE exhibited a U-shaped curve during the two growing seasons, the GPP curve had an inverted U-shape, and R_{eco} showed a trend of increased volatility during the observation period and peaked on the fourth day after harvest (figure 4). The NEE uptake peaked once during the 2013 growing season at $-4.6 \text{ g C/m}^2 \text{ d}$, but the uptake peaked twice in 2014, -4.8 and $-4.7 \text{ g C/m}^2 \text{ d}$. GPP was lower than R_{eco} early in the growing season (April in 2013 and March in 2014, table 1), and NEE was positive; the

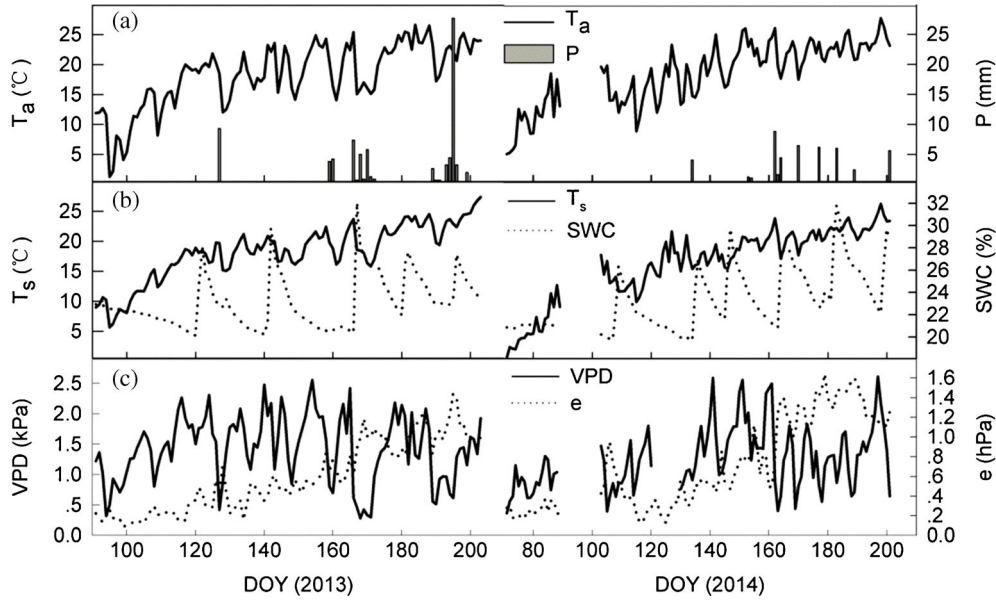


Figure 2. Variations of meteorological parameters at the study site in (left) 2013 and (right) 2014. (a) Daily mean air temperature (T_a) and precipitation (P). (b) Daily mean soil temperature (T_s) and volumetric soil-water content (SWC) at a depth of 5 cm. (c) Daily mean vapour-pressure deficit (VPD) and water-vapour pressure (e). DOY: day of year.

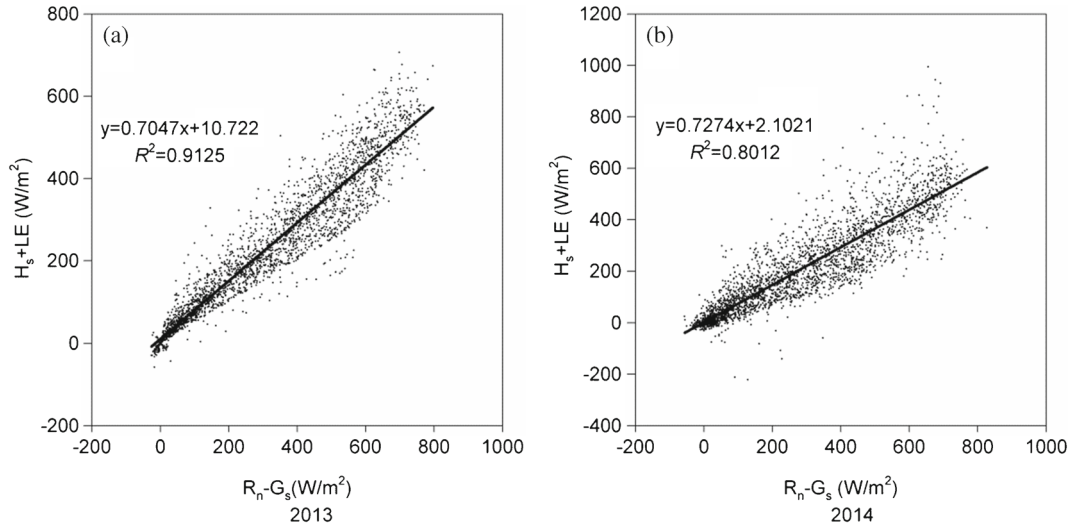


Figure 3. Regression lines of the energy balance closure and the coefficient of determination (R^2) of ($H_s + LE$ vs. $R_n - G_s$) for (a) 2013 and (b) 2014.

wheat ecosystem thus acted as a carbon source. GPP increased with the growth of the wheat and eventually exceeded R_{eco} , and NEE became negative; the ecosystem thus became a carbon sink (May and June in 2013, and April, May, and June in 2014; table 1). Most carbon was sequestered in May and June in both growing seasons, and the rate of CO₂ uptake was low in April during the 2014 growing season (table 1). The ecosystem became a carbon source again late in the growing season (July in 2013 and 2014, table 1) with the decrease in photosynthesis and increase in respiration due to the maturation of the wheat. The accumulated NEEs for the entire observation

periods were -111.6 and -142.2 g C/m² in 2013 and 2014, respectively (table 1). R_{eco} peaked on the fourth day after the wheat harvest, perhaps due to the covering of wheat straw that increased the soil temperature and thus respiration. NEE, R_{eco} , and GPP may have been over- or underestimated in 2014 due to the lack of data for 89–102 d and 121–129 d. The spring wheat ecosystem acted as a carbon sink during the growing season, and the length of the growing season may have had a significant influence on the CO₂ fluxes.

Diurnal NEE varied similarly in the months of the observation period and had a U-shaped curve, with an absorption peak near 12:00 and two emission

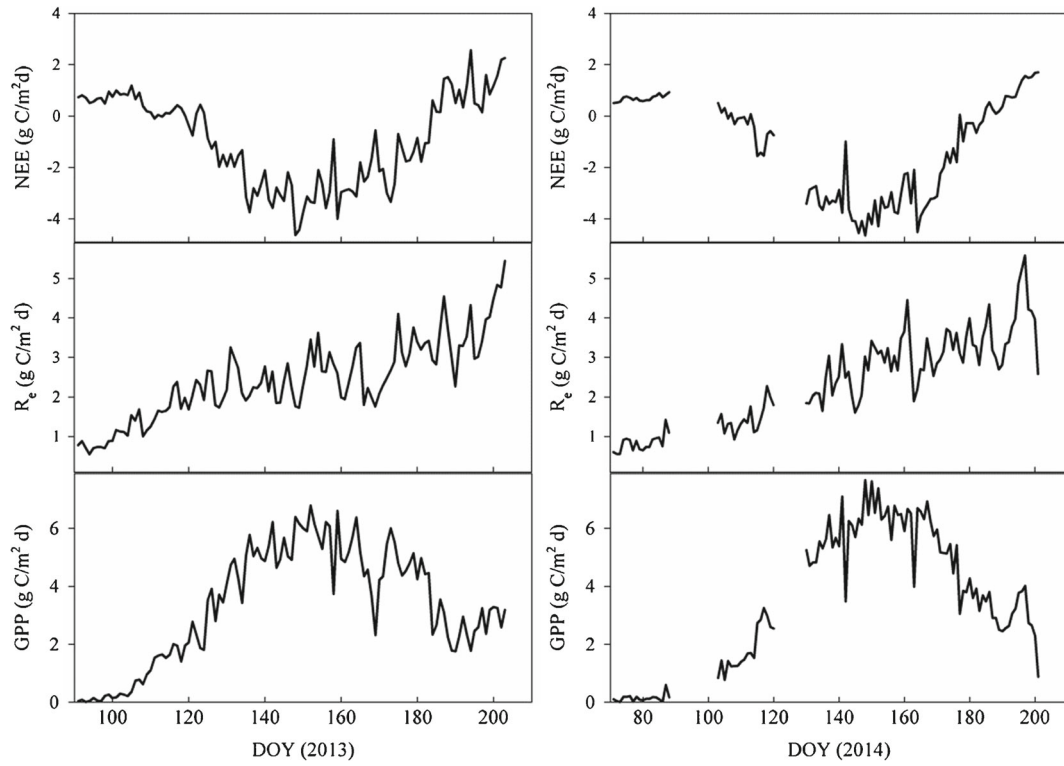


Figure 4. Dynamics of net ecosystemic CO₂ exchange (NEE), ecosystemic respiration (R_{eco}), and gross primary productivity (GPP) during the 2013 and 2014 growing season. DOY: day of year.

Table 1. Accumulated net ecosystemic CO₂ exchange (NEE), ecosystemic respiration (R_{eco}), and gross primary productivity (GPP) in different months during 2013 and 2014 growing season.

Growing season	(g C/m ²)	Months					Total
		March	April	May	June	July	
2013	NEE	–	14.691	–69.314	–69.211	12.196	–111.638
	R_{eco}	–	38.126	70.678	82.953	61.625	253.382
	GPP	–	23.766	139.992	152.165	49.429	365.351
2014	NEE	12.467	–6.778	–76.131	–75.380	3.598	–142.224
	R_{eco}	14.951	26.105	52.272	93.770	43.860	230.959
	GPP	2.484	32.883	128.403	169.150	40.262	373.182

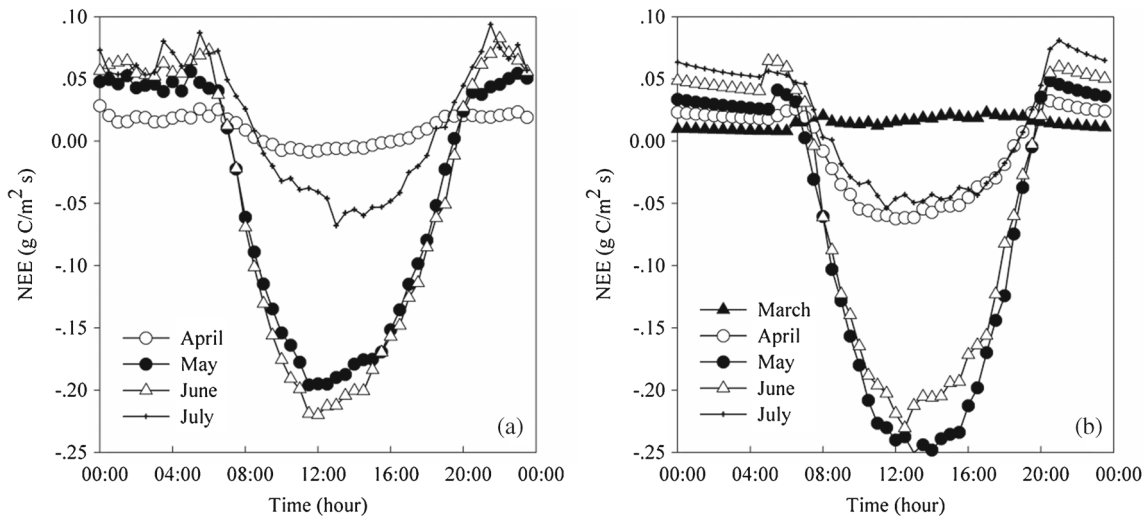


Figure 5. Diurnal net ecosystemic CO₂ exchange (NEE) in different months during the 2013 (a) and 2014 (b) growing season.

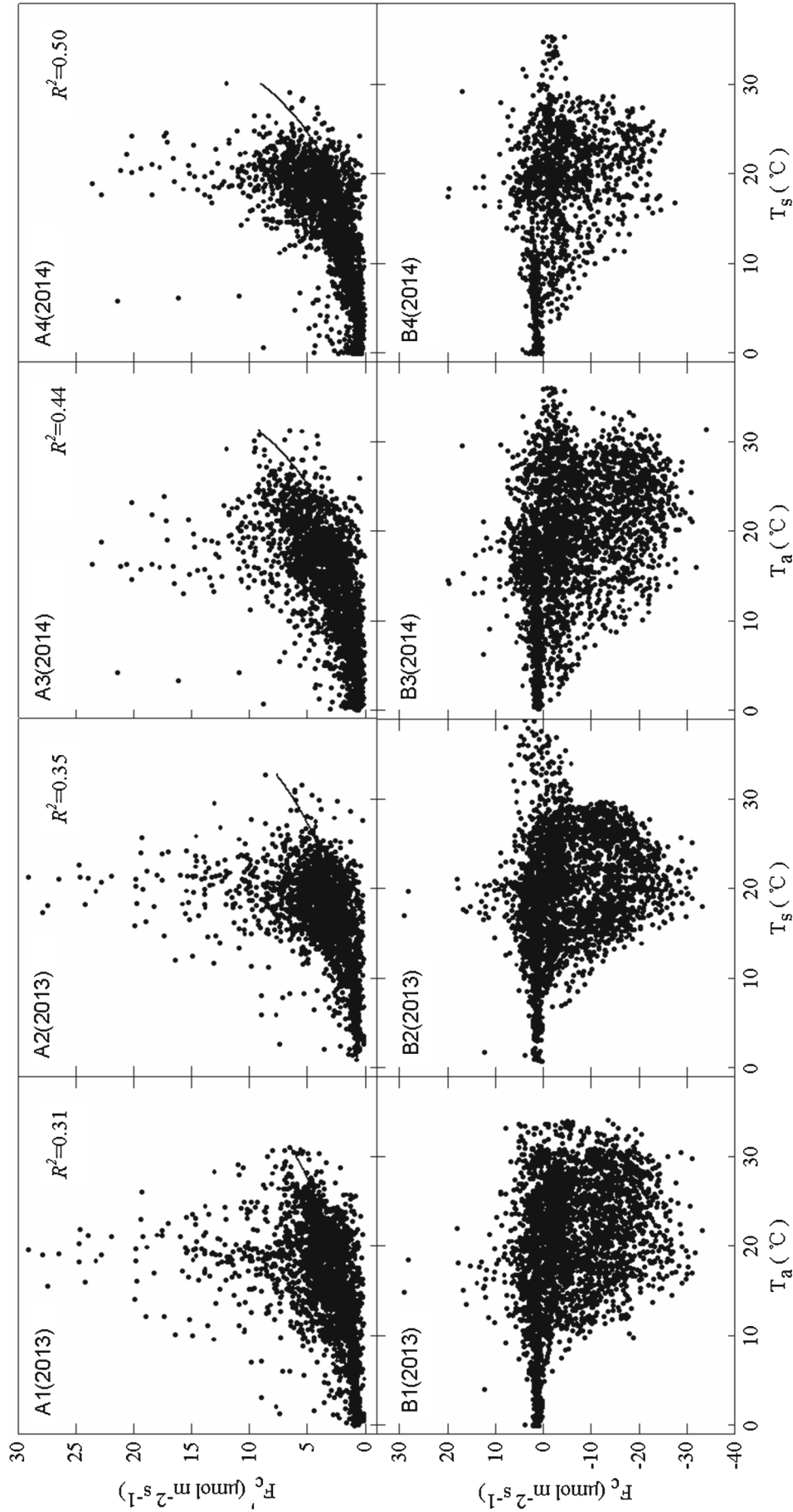


Figure 6. Response of daytime (F_c) night-time (F_c) CO₂ fluxes to daytime and night-time air temperature (T_a) and soil temperature (T_s) during 2013 and 2014 growing season.

peaks at 6:00 and 20:00, except for March in 2014 (figure 5). NEE increased after sunrise until peaking near 12:00 and then decreased, with an initial ‘trough’ between 12:00 and 14:00 known as the ‘photosynthetic lunch break phenomenon’. The value of diurnal NEE was positive in March during the 2014 growing season, with small fluctuations and no clear peak because the wheat was in the seed and seedling stages, so the plants were small and weakly photosynthetic, but respiration levels were high.

3.4 Responses of CO_2 fluxes to meteorological parameters

3.4.1 Response of CO_2 flux to temperature

The responses of daytime (F_c) and night-time (F'_c , night-time ecosystem respiration) CO_2 fluxes to T_a and T_s are shown in figure 6. The relationships between F'_c and night-time T_a and T_s showed the similar trend during the two growing seasons (figure 6A1–A4). But the coefficient of the exponential equation varied in the two growing seasons (table 2). R^2 was only 0.35 and 0.31 between F'_c and T_s and T_a in 2013 (figure 6A1, A2), respectively, and was 0.50 and 0.44 in 2014 (figure 6A3, A4), higher than in 2013 ($p < 0.001$), indicating that the variations of F'_c were sensitive to the changes in T_s and T_a at night throughout the growing season.

The relationships between F_c and T_a and T_s were also exhibited the similar variations during the two growth periods. However, F_c was not significantly correlated with daytime T_s or T_a during the two growing seasons (figure 6B1–B4).

3.4.2 Response of CO_2 flux to SWC and rainfall

The changes of SWC, precipitation and CO_2 fluxes during the 2013 and 2014 growing seasons are shown in figure 7. SWC increased substantially with irrigation, and CO_2 fluxes reached a low peak 1–2 days after irrigation. CO_2 uptake then increased. CO_2 fluxes increased in volatility with the extension of the growing season coupled with irrigation until peaking throughout the growing season before decreasing. The daily mean CO_2 fluxes decreased only with precipitation and not before a rain, and daily mean CO_2 fluxes peaked 3–6 days after a rain. Therefore, CO_2 fluxes changed more frequently when irrigation coincided with rain for irrigation or rainfall separately, suggesting that the variation of CO_2 fluxes was more complex during coincidental irrigation and rain. However, the relationship between CO_2 fluxes and SWC was not significantly correlated (figure 8A). This may be because of irrigation and/or precipitation not increased SWC, but also changed the micrometeorological that caused the result.

Table 2. Relationships between night-time CO_2 flux (F'_c , night-time ecosystemic respiration) and night-time soil temperature (T_s) at a depth of 5 cm and air temperature (T_a) at a height of 1.5 m (95% confidence level, $p < 0.001$).

Growing season	T_s	T_a
2013	$F'_c = 0.577\exp(0.095T_s)$	$F'_c = 0.835\exp(0.076T_a)$
2014	$F'_c = 0.550\exp(0.105T_s)$	$F'_c = 0.626\exp(0.097T_a)$
2013–2014	$F'_c = 0.566\exp(0.099T_s)$	$F'_c = 0.715\exp(0.086T_a)$

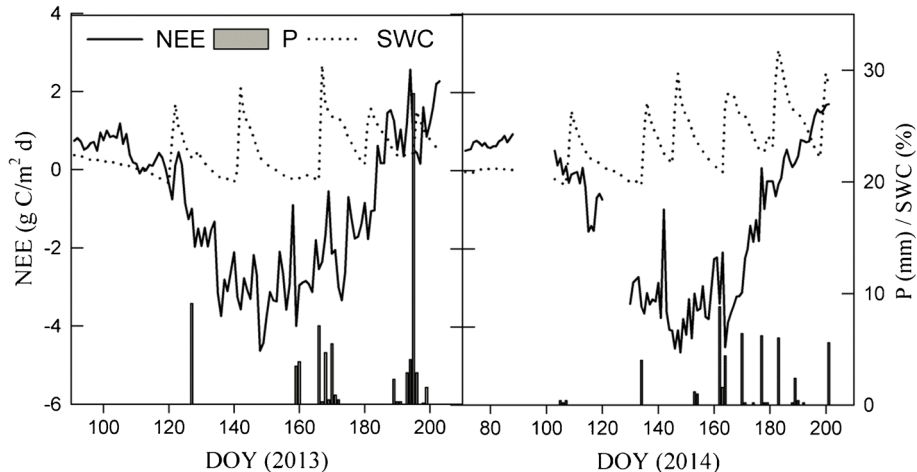


Figure 7. Changes in soil volumetric water content (SWC), precipitation (P) and CO_2 fluxes (NEE) during the two growth periods. DOY: day of year.

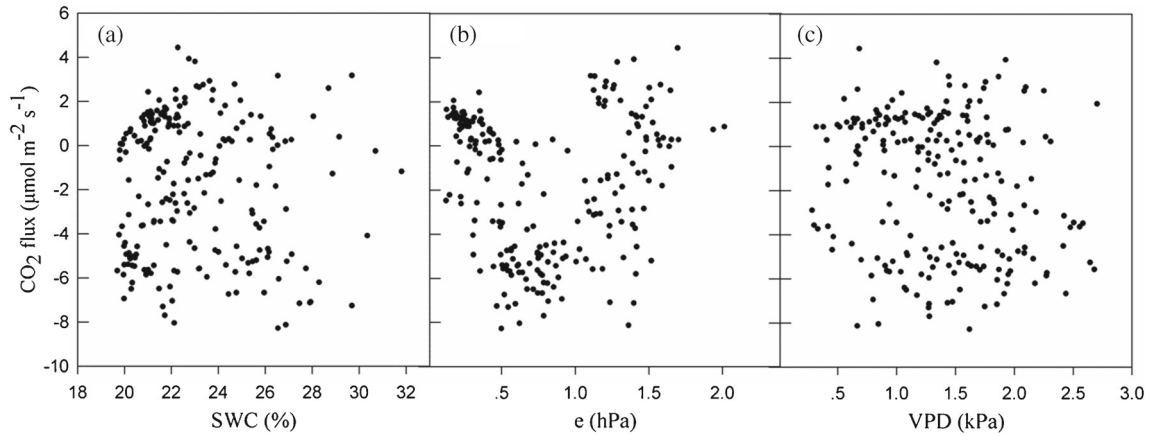


Figure 8. Dependence of daily mean CO₂ fluxes on daily mean SWC (a), e (b) and VPD (c) in the 2013 and 2014 growing season.

The dependence of daily mean CO₂ fluxes on daily mean e and VPD during the 2013 and 2014 growing seasons is shown in figure 8(b, c). Interestingly, CO₂ fluxes were not significantly correlated with either e or VPD.

4. Discussion

4.1 Energy balance

Energy imbalance is a widespread phenomenon in various ecosystems around the world. Wilson *et al.* (2002) reported that the mean imbalance at 22 sites with various functional types of vegetation, including forests, grassland, and cropland, was near 20%, and Stoy *et al.* (2013) reported a mean EBC of 0.84, with a range of 0.28–1.67, for plant functional types including forests, wetland, savannah, and cropland. In our study, the mean EBCs and EBRs were 70.5% and 0.74 in 2013 and 72.7% and 0.73 in 2014, respectively. The lack of EBC can be partially attributed to an underestimation of the turbulent heat fluxes and/or an overestimation of the available energy (Wilson *et al.* 2002; Vote *et al.* 2015). Furthermore, ignoring the heat stored in soil, plant biomass and canopy air mass, the biochemical photosynthetic energy consumption can produce low estimates of EBC (Kilinc *et al.* 2012). Oliphant *et al.* (2004) reported that soil heat storage, biomass heat storage, and sensible heat in the air column below the EC system contributed significantly to the diurnal pattern of heat storage, and soil heat storage varied significantly on a seasonal scale. Estimates of surface EBC improve with the inclusion of the heat stored in the soil (Jacobs *et al.* 2007). Our average EBC was thereby enhanced by 2–3% due to including soil heat storage. However, Xu *et al.* (2013) reported that the inclusion of soil heat storage in agricultural

fields (wheat, corn, and cotton) could increase the monthly EBC by 4–11% and the annual EBC by 3–5%. The inclusion of soil heat storage also improved the EBC by 1.59% in a subalpine meadow (Wang and Zhang 2011), 9% in grassland (Jacobs *et al.* 2007), and 6–7% in desert grassland (Zuo *et al.* 2010). These differences may be due to differences in the flux of heat in different types of soil. Soil bulk density and surface temperature should also be included.

4.2 CO₂ fluxes

The annual characteristics of the CO₂ fluxes had U-shaped curves during the growing seasons, with one absorption peak in 2013 and two peaks in 2014. The wheat ecosystem acted as a CO₂ sink during the growing period and then became a CO₂ source after the wheat was harvested. This result is consistent with those for other agricultural ecosystems (Lei and Yang 2010; Wang *et al.* 2013a). The measured CO₂ fluxes varied between the two growing seasons depending on changes in the vegetative and meteorological parameters. The maximum rates of CO₂ uptake were -4.6 and -4.8 g C/m²d in 2013 and 2014, respectively, and the diurnal pattern of mean CO₂ flux for daytime uptake and night-time release was evident. These differences may have been caused by such factors as irrigation (four times during the 2013 growing season and five in 2014), environment, management (different sowing and harvest times), photosynthetic activation, and the period of observation. We calculated the daily (table 3 and figure 5) and monthly (table 1) NEEs during both growing seasons to analyse the influence of the length of the growth period on the CO₂ fluxes. The June data indicated that NEE was higher in 2014 than 2013. Some data for 2014 were missing, but the total NEE, GPP, and R_{eco}

were still higher in 2014 than 2013 (figure 4 and table 1), indicating that an extended growth period may increase the amount of CO₂ absorbed. However, further researches should be carried out to confirm whether an extension of spring wheat growth period be beneficial for the absorption of CO₂.

Diurnal CO₂ fluxes varied similarly in different months, except for March in the 2014 growing season, with a ‘photosynthetic lunch break’ from 12:00 to 14:00. This phenomenon was consistent with previous findings in a variety of vegetation (Wang et al. 2006; Grassi et al. 2009; Wagle et al. 2015). The mid-day depression of photosynthesis may be caused by stomata closure due to high VPD and temperature, even when soil is well irrigated (Wang et al. 2006). Tang et al. (1986), however, reported that mid-day depression of photosynthesis did not occur in wheat under suitable and stable conditions.

4.3 Influence of meteorological parameters on CO₂ fluxes

Photosynthesis and respiration, two important processes in terrestrial ecosystems, have strong influences on CO₂ fluxes. Net CO₂ flux decreases as photosynthesis increases and *vice versa* (Chen et al. 2014). The measured CO₂ flux in our study varied throughout the two growing seasons depending on the stage of development of the wheat and on changes of the meteorological conditions.

Temperature strongly influences soil/ecosystemic respiration. Night-time CO₂ flux is equivalent to ecosystemic respiration because photosynthesis does not occur at night (Chen et al. 2014). In our study, night-time CO₂ flux was exponentially dependent on T_a and T_s (figure 6A1–A4 and table 2). An exponential relationship between night-time CO₂ flux and air and soil temperatures has been previously reported (Suyker et al. 2004; Wang et al. 2013a; Chen et al. 2014; Vote et al. 2015). The daytime CO₂ flux, however, was not significantly correlated with either T_a or T_s (figure 6B1–B4), as also

previous report (Wang et al. 2013a; Chen et al. 2014). Maybe, these variations in daytime CO₂ fluxes are primarily controlled by photosynthetically active radiation (PAR) and LAI (Suyker et al. 2004).

We also found no correlation between CO₂ flux and volumetric SWC in either daytime or nighttime, perhaps because SWC (>19%) was not a limiting factor during the study period. This result was similar to those in previous studies (Maljannen et al. 2001; Chen et al. 2014). However, CO₂ fluxes fluctuated strongly, during the active growth of the wheat during rains and periods of irrigation, especially rains. NEE decreased 1–2 days after irrigation. NEE decreased after a rain, perhaps due to the dramatically increased R_{eco} after the rain events occurred. There are several reasons for the NEE decrease after rain. Firstly, the soil aggregates which protect soil organic matter may break down by the sudden wetting events, thus increasing the concentration of available substrates and enhancing the microbial activities (Denef et al. 2001); secondly, the infiltrating water may replace the soil CO₂ through physical displacement (Orchard and Cook 1983); last, the lysis of dead microbial cells under wetting of dry soils can induce an increase in the availability of organic substrates, which greatly stimulate the activity of surviving microbes (Kieft et al. 1987; Broken and Matzner 2009). These biological processes usually occurred within a few hours after the precipitation and release amount of CO₂ to the atmosphere in a short time, thus NEE reduced. Wang et al. (2013b) reported that daily CO₂ fluxes were significantly affected by daily rainfall >5 mm and that ecosystemic respiration peaked within 1–2 days after a rain. Daily mean CO₂ fluxes in our study peaked 3–6 days after precipitation. Irrigation and precipitation generally complicated the response of CO₂ flux to other meteorological parameters. Further studies of the response of CO₂ fluxes to volumetric SWC will thus be very important, especially during periods of irrigation and precipitation. We found no correlation between CO₂ fluxes and VPD or e (figure 8).

Table 3. Accumulated daily average net ecosystemic CO₂ exchange (NEE), ecosystemic respiration (R_{eco}), and gross primary productivity (GPP) in different months during 2013 and 2014 growing season (mean \pm SD).

Growing season	g C/m ² d	Month				
		March	April	May	June	July
2013	NEE	–	0.499 \pm 0.375	–2.236 \pm 1.277	–2.307 \pm 0.903	0.883 \pm 0.914
	R_{eco}	–	1.271 \pm 0.481	2.280 \pm 0.399	2.765 \pm 0.596	3.668 \pm 0.765
	GPP	–	0.792 \pm 0.726	4.516 \pm 1.260	5.072 \pm 0.959	2.806 \pm 0.727
2014	NEE	0.693 \pm 0.115	–0.377 \pm 0.599	–3.461 \pm 0.756	–2.513 \pm 1.264	0.703 \pm 0.689
	R_{eco}	0.831 \pm 0.213	1.450 \pm 0.338	2.376 \pm 0.543	3.216 \pm 0.516	3.724 \pm 0.818
	GPP	0.138 \pm 0.128	1.827 \pm 0.756	5.837 \pm 0.958	5.638 \pm 1.140	3.021 \pm 0.732

5. Conclusions

Continuous exchanges of energy and CO₂ were measured by EC in a field of spring wheat throughout two growing seasons in a typical desert-oasis in the middle reaches of the Heihe River in northwestern China. The wheat ecosystem had distinct dynamics of CO₂ fluxes. Total NEE was -111.6 and -142.2 g C/m² during the observation periods of 2013 and 2014, respectively. The wheat ecosystem acted as a CO₂ sink during the growing season but became a CO₂ source after the harvest. A 'photosynthesis lunch break' was found from 12:00 to 14:00. The CO₂ fluxes were exponentially correlated with air and soil temperature at night but were not correlated in daytime. The CO₂ fluxes were also not correlated with SWC, VPD, or *e*. Irrigation and precipitation complicated the response of the CO₂ fluxes to SWC, and CO₂ emission (absolute value) decreased after rain. However, the mechanism of precipitation effect on CO₂ fluxes should be deeply studied.

Acknowledgements

This study was supported by the National Natural Science Foundation of China (No. 91025018). Thanks go to the staff of the Linze Inland River Basin Research Station, Chinese Ecosystem Research Network.

References

- Admiral S W, Laffleur P M and Roulet N T 2006 Controls on latent heat flux and energy partitioning at a peat bog in eastern Canada; *Agric. For. Meteorol.* **140** 308–321.
- Aubinet M, Grelle A, Ibrom A, Rannik Ü, Moncrieff J, Foken T, Kowalski S, Martin P H, Berbigier P, Bernhofer C, Clement R, Elbers J, Granier A, Grünwald T, Morgenstern K, Pilegaard K, Rebmann C, Snijders W, Valentini R and Vesala T 2000 Estimates of the annual net carbon and water exchange of forests: The EUFORFLUX methodology; *Adv. Ecol. Res.* **30** 113–175.
- Broken W and Matzner E 2009 Reappraisal of drying and wetting effects on C and N mineralization and fluxes in soils; *Global Change Biol.* **15** 808–824.
- Chen H Q, Fan M S, Kuzyakov Y, Billen N and Karl S 2014 Comparison of net ecosystem CO₂ exchange in cropland and grassland with an automated closed chamber system; *Nutr. Cycl. Agroecosys.* **98** 113–124.
- Cheng G D, Xiao D N and Wang G X 1999 On the characteristics and building of landscape ecology in arid area; *Adv. Earth Sci.* **14** 11–15 (in Chinese).
- Denef K, Six J, Bossuyt H, Frey S D, Elliott E T, Merckx R and Paustian K 2001 Influence of dry-wet cycles on the interrelationship between aggregate, particulate organic matter, and microbial community dynamics; *Soil Biol. Biochem.* **33** 1599–1611.
- Falge E, Baldocchi D, Olson R, Anthoni P, Aubinet M, Bernhofer C, Burba G, Ceulemans R, Clement R, Dolman H, Granier A, Gross P, Gtünwald T, Hollinger D, Jensen N O, Katul G, Keronen P, Kowalski A, Lai C T, Law B E, Meyers T, Moncrieff J, Moors E, Munger J W, Pilegaard K, Rannik Ü, Rebmann C, Suyker A, Tenhunen J, Tu K, Verma S, Vesala T, Wilson K and Wofsy S 2001 Gap filling strategies for defensible annual sums of net ecosystem exchange; *Agric. For. Meteorol.* **107** 43–69.
- Foley J A, DeFries R, Asner G P, Barford C, Bonan G, Carpenter S R, Chapin F S, Coe M T, Daily G C, Gibbs H K, Helkowski J H, Holloway T, Howard E A, Kucharik C J, Monfreda C, Patz J A, Prentice I C, Ramankutty N and P K Snyder 2005 Global consequences of land use; *Science* **309** 570–574.
- Grassi G, Ripullone F, Borghetti M, Raddi S and Magnani F 2009 Contribution of diffusional and non-diffusional limitations to midday depression of photosynthesis in *Arbutus unedo* L; *Trees* **23** 1149–1161.
- Hanks R J and Ashcroft L G 1980 *Applied Soil Physics: Soil Water and Temperature Application*; Springer-Verlag, 159p.
- Hunt J E, Kelliher F M, Mcseveny T M, Ross D J and Whitehead D 2004 Long-term carbon exchange in a sparse, seasonally dry tussock grassland; *Global Change Biol.* **10** 1785–1800.
- Intergovernmental Panel on Climate Change 2007 Climate Change 2007: Synthesis Report; Contribution of Working Groups I, II and III to the Fourth Assessment Report of the Intergovernmental Panel on Climate Change, Geneva, Switzerland.
- Ivans S, Hipps L, Leffler A J and Ivans C Y 2006 Response of water vapour and CO₂ fluxes in semiarid lands to seasonal and intermittent precipitation; *J. Hydrometeorol.* **7** 955–1010.
- Jacobs A F G, Heusinkveld B G and Holtslag A A M 2007 Towards closing the surface energy budget of a mid-latitude Grassland; *Bound.-Layer Meteor.* **126** 125–136.
- Jiang Y, Wang P, Xu X D and J H Zhang 2014 Dynamics of carbon fluxes with responses to vegetation, meteorological and terrain factors in the south-eastern Tibetan Plateau; *Environ. Earth Sci.* **72** 4551–4565.
- Jing Y L, Wang A Z, Guan D X, Wu J B, Yuan F H and Jin C J 2014 Carbon dioxide fluxes over a temperate meadow in eastern Inner Mongolia, China; *Environ. Earth Sci.* **72** 4401–4411.
- José S J, Montes R and Nikonova N 2007 Seasonal patterns of carbon dioxide, water vapour and energy fluxes in pineapple; *Agric. For. Meteorol.* **147** 16–34.
- Khan S and Hanjra M A 2009 Footprints of water and energy inputs in food production – global perspectives; *Food Policy* **34** 130–140.
- Kieft T L, Soroker E and Firestone M K 1987 Microbial biomass response to a rapid increase in water potential when dry soil is wetted; *Soil Biol. Biochem.* **19** 119–126.
- Kilinc M, Beringer J, Hutley L B, Haverd V and Tapper N 2012 An analysis of the surface energy budget above the world's tallest angiosperm forest; *Agric. For. Meteorol.* **166–167** 23–31.
- Lei H M and Yang D W 2010 Seasonal and inter annual variations in carbon dioxide exchange over a cropland in the North China Plain; *Global Change Biol.* **16** 44–57.
- Leuning R, Cleugh H A, Zegelin S J and Hughes D 2005 Carbon and water fluxes over a temperate eucalyptus forest and a tropical wet/dry savanna in Australia: Measurements and comparison with DODIS remote sensing estimates; *Agric. For. Meteorol.* **129** 151–173.

- Li D F and Shao M A 2014 Temporal stability of soil water storage in three landscapes in the middle reaches of the Heihe River, northwestern China; *Environ. Earth Sci.*, doi: [10.1007/s12665-014-3604-z](https://doi.org/10.1007/s12665-014-3604-z).
- Li X G, Li F M, Rengel Z, Bhupinderpal S and Wang Z F 2006 Cultivation effects on temporal changes of organic carbon and aggregate stability in desert soils of Hexi Corridor region in China; *Soil Till. Res.* **91** 22–29.
- Lloyd J and Taylor J A 1994 On the temperature dependence of soil respiration; *Funct. Ecol.* **8** 315–323.
- Mahrt L 1998 Flux sampling errors for aircraft and towers; *J. Atmos. Ocean. Technol.* **15** 416–429.
- Maljanen M, Martikainen P, Walden J and Silvola J 2001 CO₂ exchange in an organic field growing barley or grass in eastern Finland; *Global Change Biol.* **7** 679–692.
- Morgan J A, LeCain D R, Pendall E, Blumenthal D M, Kimball B A, Carrillo Y, Williams D G, Heisler-White J, Dijkstra F A and West M 2011 C₄ grasses prosper as carbon dioxide eliminates desiccation in warmed semi-arid grassland; *Nature* **476** 202–206.
- Ohta T, Kotani A, Iijima Y, Maximov T C, Ito S, Hanamura M, Kononov A V and Maximov A P 2014 Effects of water-logging on water and carbon dioxide fluxes and environmental variables in a Siberian larch forest, 1998–2011; *Agric. For. Meteorol.* **188** 64–75.
- Oliphant A J, Grimmond C S B, Zutter H N, Schmid H P, Su H B, Scott S L, Offerle B, Randolph J C and Ehman J 2004 Heat storage and energy balance fluxes for a temperate deciduous forest; *Agric. For. Meteorol.* **126** 185–201.
- Orchard V A and Cook F J 1983 Relationship between soil respiration and soil moisture; *Soil Biol. Biochem.* **15** 447–453.
- Patil M N, Dharmaraj T, Waghmare R T, Prabha T V and Kulkarni J R 2014 Measurements of carbon dioxide and heat fluxes during monsoon-2011 season over rural site of India by eddy covariance technique; *J. Earth Syst. Sci.* **123** 177–185.
- Pielke R A, Avissar R, Ranpach M, Dolman J, Zeng X B and Denning S 1998 Interactions between the atmosphere and terrestrial ecosystem: Influence on weather and climate; *Global Change Biol.* **4** 461–475.
- Posse G, Richter K, Lewczuk N, Cristiano P, Gattinoni N, Rebella C and Achkar A 2014 Attribution of carbon dioxide fluxes to crop types in a heterogeneous agricultural landscape of Argentina; *Environ. Model Assess.* **19** 361–372.
- Reichstein M, Tenhunen J D, Rouspard O, Ourcival J, Ranbal S, Miglietta F, Peressotti A, Pecchian M, Tirone G and Valentini R 2002 Severe drought effects on ecosystem CO₂ and H₂O fluxes at three Mediterranean evergreen sites: Revision of current hypotheses?; *Global Change Biol.* **8** 999–1017.
- Rotenberg E and Yakir D 2010 Contribution of semi-arid forests to the climate system; *Science* **327** 451–454.
- Schimel D S 2010 Drylands in the earth system; *Science* **327** 418–419.
- Schmid H P, Grimmond C S B, Cropley F, Offerle B and Su H B 2000 Measurement of CO₂ and energy fluxes over a mixed hardwood forest in the mid-western United States; *Agric. For. Meteorol.* **103** 357–374.
- Scott R L, Serrano-Ortiz P, Domingo F, Hamerlynck E P and Kowalski A S 2012 Commonalities of carbon dioxide exchange in semi-arid regions with monsoon and Mediterranean climates; *J. Arid Environ.* **84** 71–79.
- Spiertz H 2012 Avenues to meet food security. The role of agronomy on solving complexity in food production and resource use; *Eur. J. Agron.* **43** 1–8.
- Stoy P C, Mauder M, Foken T, Marcolla B, Boegh E, Ibrom A, Arain M A, Arneth A, Aurela M, Bernhofe C, Cescatti A, Dellwik E, Duce P, Gianelle D, Van Gorsel E, Kiely G, Knohl A, Margolis H, McCaughey H, Merbold L, Montagnani L, Papale D, Reichstein M, Saunders M, Serrano O P, Scottocornola M, Spano D, Vaccari F and Varlagin A 2013 A data-driven analysis of energy balance closure across FLUXNET research sites: The role of landscape scale heterogeneity; *Agric. For. Meteorol.* **171–172** 137–152.
- Suyker A E, Verma S B, Burba G G, Arkebauer T J, Walters D T and Hubbard K G 2004 Growing season carbon dioxide exchange in irrigated and rainfed maize; *Agric. For. Meteorol.* **124** 1–13.
- Tang H S, Liu T H and Yu Y B 1986 Studies on ecological factors of the photosynthesis ‘NAP’ in wheat; *Acta Eco. Sin.* **6** 128–132 (in Chinese).
- Trenberth K E, Fasullo J T and Kiehl J 2009 Earth’s global energy budget; *Am. Meteorol. Soc.* **3** 311–323.
- Tsai J L, Tsuang B J, Lu P S, Yao M H and Shen Y 2007 Surface energy components and land characteristics of a rice paddy; *J. Appl. Meteorol. Clim.* **11** 1870–1900.
- Tyagi B, Satyanarayana A N V, Rajvashi R K and Mandal M 2014 Surface energy exchanges during pre-monsoon thunderstorm activity over a Tropical station Kharagpur; *Pure Appl. Geophys.* **171** 1445–1459.
- Vote C, Hall A and Charlton P 2015 Carbon dioxide, water and energy fluxes of irrigated broad-acre crops in an Australian semi-arid climate zone; *Environ. Earth. Sci.* **73** 449–465.
- Wagle P, Xiao X M and Suyker A E 2015 Estimation and analysis of gross primary production of soybean under various management practices and drought conditions; *J. Photogramm. Remote Sens.* **99** 70–83.
- Wang R Y and Zhang Q 2011 An assessment of storage terms in the surface energy balance of a sub-alpine meadow in northwest China; *Adv. Atmos. Sci.* **28** 691–698.
- Wang J, Yu Q, Li J, Li L H, Li X G, Yu G R and Sun X M 2006 Simulation of diurnal variations of CO₂, water and heat fluxes over winter wheat with a model coupled photosynthesis and transpiration; *Agric. For. Meteorol.* **137** 194–219.
- Wang W, Liao Y C, Wen X X and Guo Q 2013a Dynamics of CO₂ fluxes and environmental response in the rain-fed winter wheat ecosystem of the Loess Plateau, China; *Sci. Total Environ.* **461–462** 10–18.
- Wang W, Liao Y C and Guo Q 2013b Responses of ecosystem CO₂ fluxes to rainfall events in rain-fed winter wheat agro-ecosystem; *J. Food. Agric. Environ.* **11** 982–986.
- Wilson K B and Baldocchi D D 2000 Seasonal and inter-annual variability of energy fluxed over a broadleaved temperate deciduous forest in North America; *Agric. For. Meteorol.* **100** 1–18.
- Wilson K, Goldstein A, Falge E, Aubinet M, Baldocchi E, Berbigier P, Bernhofer C, Ceulemans R, Dolman H, Field C, Grelle A, Ibrom A, Law B E, Kowalski A, Meyers T, Moncrieff J, Monson R, Oechel W, Tenhunen J, Valentini R and Verma S 2002 Energy balance closure at FLUXNET sites; *Agric. For. Meteorol.* **113** 223–243.
- Xu Z W, Liu S M, Xu T R and Ding C 2013 The observation and calculation method of soil heat flux and its impact on the energy balance closure; *Adv. Earth Sci.* **28** 875–889 (in Chinese).
- Yu Q, Wu W, Yang P Li Z, Xiong W and Tang H 2012 Proposing an interdisciplinary and cross-scale framework

Energy and CO₂ fluxes in spring wheat over northwestern China

- for global change and food security researches; *Agric. Ecosyst. Environ.* **156** 57–71.
- Yuan G F, Zhang P, Shao M A, Luo Y and Zhu X C 2014 Energy and water exchanges over a riparian *Tamarix* spp. stand in the lower Tarim River basin under a hyper-arid climate; *Agric. For. Meteorol.* **194** 144–154.
- Zhang P P and Shao M A 2013 Temporal stability of surface soil moisture in a desert area of northwestern China; *J. Hydrol.* **505** 91–101.
- Zeri M, Sá L D A, Manzi A O, Araújo A C, Aguiar R G, Randow C, Sampaio G, Cardoso F L and Nobre C A 2014 Variability of carbon and water fluxes following climate extremes over a Tropical forest in southwestern Amazonia; *PLOS ONE* **9** 1–12.
- Zuo J Q, Wang J M, Huang J P, Li W J, Wang G Y and Ren H L 2010 Estimation of ground heat flux of a semi-arid grassland and its impact on the surface energy budget; *Plateau Meteorol.* **29** 840–848 (in Chinese).

MS received 2 March 2016; revised 21 August 2016; accepted 30 August 2016

Corresponding editor: K KRISHNAMOORTHY